Birbeck Granules Are Subdomains of Endosomal Recycling Compartment in Human Epidermal Langerhans Cells, Which Form Where Langerin Accumulates

Ray Mc Dermott,*[†] Umit Ziylan,[†‡] Danièle Spehner,[‡] Huguette Bausinger,[‡] Dan Lipsker,[‡] Mieke Mommaas,[§] Jean-Pierre Cazenave,[‖] Graça Raposo,[¶] Bruno Goud,* Henri de la Salle,[‡] Jean Salamero,* and Daniel Hanau[‡#]

Unité Mixte de Recherche 144 Centre National de la Recherche Scientifique-Institut Curie, *Laboratoire Mécanismes Moléculaires du Transport Intracellulaire and [¶]Laboratoire de Microscopie Electronique, Institut Curie, 75248 Paris, France; [‡]Institut National de la Santé et de la Recherche Médicale EP 99–08 Biologie des Cellules Dendritiques Humaines and [‖]Institut National de la Santé et de la Recherche Médicale U 311, Etablissement Français du Sang-Alsace, 67065 Strasbourg, France; and [§]Department of Dermatology and Center for Electron Microscopy, Leidem University Medical Center, 2300 RA Leiden, The Netherlands

Birbeck granules are unusual rod-shaped structures specific to epidermal Langerhans cells, whose origin and function remain undetermined. We investigated the intracellular location and fate of Langerin, a protein implicated in Birbeck granule biogenesis, in human epidermal Langerhans cells. In the steady state, Langerin is predominantly found in the endosomal recycling compartment and in Birbeck granules. Langerin internalizes by classical receptor-mediated endocytosis and the first Birbeck granules accessible to endocytosed Langerin are those connected to recycling endosomes in the pericentriolar area, where Langerin accumulates. Drug-induced inhibition of endocytosis results in the appearance of abundant open-ended Birbeck granule-like structures appended to the plasma membrane, whereas inhibition of recycling induces Birbeck granules to merge with a tubular endosomal network. In mature Langerhans cells, Langerin traffic is abolished and the loss of internal Langerin is associated with a concomitant depletion of Birbeck granules. Our results demonstrate an exchange of Langerin between early endosomal compartments and the plasma membrane, with dynamic retention in the endosomal recycling compartment. They show that Birbeck granules are not endocytotic structures, rather they are subdomains of the endosomal recycling compartment that form where Langerin accumulates. Finally, our results implicate ADP-ribosylation factor proteins in Langerin trafficking and the exchange between Birbeck granules and other endosomal membranes.

INTRODUCTION

Langerhans cells (LCs), the representatives of the dendritic cell lineage in the epidermis and mucosal tissues, capture antigen in the skin before migrating to the T-cell–dependent areas of draining lymph nodes. During this migration, they undergo a maturation process that allows them to present antigens to naive T cells (Kripke *et al.*, 1990; Moll *et al.*, 1993). Notably, Langerhans cells are the only epidermal cells to constitutively express major histocompatibility complex class II molecules (Klareskog *et al.*, 1977; Rowden *et al.*, 1977), CD1a molecules (Fithian *et al.*, 1981), and Langerin (Valladeau *et al.*, 2000) at their cell surface. In addition, Langerhans cells differ ultrastructurally from other dendritic cells through the presence of Birbeck granules (BGs), distinctive rod-shaped structures of variable length with a central, periodically striated lamella (Birbeck *et al.*, 1961).

Despite the use of "dynamic" electron microscope studies (reviewed in Schuler *et al.*, 1991), Birbeck granules remain enigmatic. Specifically, conflicting theories exist regarding

their derivation and function. The secretion/exocytosis theory suggests an intracellular origin from either the Golgi apparatus or endosomes. In this model, Birbeck granules would take up intracellular ligands and transport them either to the cell surface or an unknown intracellular destination (Zelickson, 1966; Wolff, 1967; Hanau *et al.*, 1987). Alternatively, the endocytosis theory posits that Birbeck granules originate from the cell membrane, during receptor-mediated endocytosis, as a prolongation of coated pits that pinch off to form intracellular Birbeck granules. Once formed, these structures would potentially deliver ligands to endosomal, prelysosomal, and lysosomal compartments (Ishii *et al.*, 1984; Takigawa *et al.*, 1985; Bartosik, 1992).

The recent characterization of Langerin has provided some insight into the biogenesis of Birbeck granules. Langerin is a transmembrane type II Ca^{2+}-dependent lectin with a single carbohydrate recognition domain displaying mannose-binding specificity and an intracellular proline-rich motif (Valladeau *et al.*, 2000). The presence of Langerin is sufficient to promote the appearance of structures similar to Birbeck granules in murine fibroblastic cells (Valladeau *et al.*, 2000), suggesting that it may equally be involved in their formation in human Langerhans cells.

In an attempt to resolve some of the persistent issues surrounding the origin and function of these unusual cell-specific structures, we undertook a study of Birbeck granules in human epidermal Langerhans cells. Given the implication of Langerin in their biogenesis, we specifically studied the relationship between Langerin and Birbeck granules in these cells. Our results demonstrate that in freshly isolated Langerhans cells, recycling Langerin is dynamically retained in the endosomal recycling compartment and that Birbeck granules form where Langerin accumulates. They also demonstrate that Birbeck granules constitute a subdomain of the endosomal recycling compartment.

MATERIALS AND METHODS

Antibodies and Reagents

Mouse monoclonal antibodies (mAbs) were as follows: anti-lag (IgG1, recognizing an intracellular epitope of Langerin; kindly provided by Dr. Sadao Imamura, Kyoto University, Sakyo-ku, Kyoto, Japan) (Kashihara *et al.*, 1986; Valladeau *et al.*, 2000), DCGM4 (IgG1, recognizing an extracellular epitope of Langerin; Immunotech, Marseille, France) (Valladeau *et al.*, 1999), L243 (IgG2a, anti-DR$\alpha\beta$ dimmers; BD Biosciences, San Jose, CA), fluorescein isothiocyanate (FITC)-conjugated H1149 (IgG1, anti-CD1a; BD PharMingen, San Diego, CA), H5C6 (IgG1, anti-CD63; kindly provided by Dr. François Lanza, EFS-Alsace, Strasbourg), tetramethylrhodamine B isothiocyanate (TRITC)-conjugated Phalloidin (Sigma, St. Louis, MO), and H4B4 (IgG1, anti-Lamp-2 [CD107b], BD PharMingen). Rabbit anti-EEA1 antiserum (Simonsen *et al.*, 1998) was a generous gift of Dr. Harald Steinmark, (EMBL, Heidelberg, Germany). CTR433, a mouse mAb recognizing a *cis*/medial Golgi antigen (Jasmin *et al.*, 1989) was provided by Dr. Michel Bornens (Institut Curie, Paris, France). A polyclonal rabbit anti-Rab11 antibody was raised against full-length recombinant Rab11 expressed in *Escherichia coli* and affinity purified essentially as described previously (Martinez *et al.*, 1994). L243 and H5C6 were directly coupled to cyanin 3 by using a CY3-link kit (Amersham France, Les Ullis, France) according to the manufacturer's instructions. FITC-conjugated mouse IgG1 (BD PharMingen) was used as an isotype control in cytometric analyses. An FITC-conjugated, affinity-isolated F(ab')$_2$ fraction of a sheep anti-mouse Ig antibody (Silenius, Hawthorn, Victoria, Australia)

was used for indirect immunofluorescence labeling procedures in fluorescence-activated cell sorting (FACS) analyses. Texas Red-conjugated donkey anti-rabbit IgG F(ab')$_2$ fragments and Texas Red or FITC-conjugated donkey anti-mouse IgG F(ab')$_2$ fragments (Jackson Immunoresearch, West Grove, PA) were used for indirect immunofluorescence staining procedures in confocal microscopy. Gold-conjugated Fab fragments of the anti-CD1a mAb BL6 (Immunotech) (anti-CD1a-Au) for electron microscopy were obtained from Aurion (Wageningen, The Netherlands). The anti-Langerin mAb DCGM4 was labeled with 10-nm gold particles (Goldsols EM-10 nm; Aurion) (DCGM4-Au) as previously reported (Hanau *et al.*, 1987). Finally, fixation of DCGM4 on ultrathin cryosections was revealed by indirect immunogold staining with rabbit anti-mouse IgG (Dakopatts, Carpinteria, CA) followed by protein A-colloidal gold. Isotype-matched irrelevant antibodies served as controls.

Recombinant human granulocyte-macrophage colony-stimulating factor (GM-CSF) was obtained from PeproTech (Rocky Hill, NJ) and recombinant human tumor necrosis factor-α (TNF-α) from Sigma. Latrunculin A (L-12370) was provided by Molecular Probes (Eugene, OR). Cytochalasin D (C 8273), horseradish peroxidase (HRP) type II (P-8250), diaminobenzidine (DAB) (D-5905), and brefeldin A (BFA) (B-7651) were from Sigma. BFA and cytochalasin D were stored at $-20°C$ in ethanol as a 5 and 1 mg/ml stock solution, respectively.

Preparation and Culture of Epidermal Cells

Cell suspensions were prepared from normal human skin taken from patients undergoing abdominal plastic surgery, as previously described (Hanau *et al.*, 1987). These suspensions initially contained 0.5–2% freshly isolated (Fi) LCs and were enriched in LCs by gradient centrifugation on Lymphoprep (Flobio SA, Courbevoie, France) giving an LC yield typically 30–50% of the final cell population.

Cultures of epidermal cell suspensions enriched in LCs were established in RPMI 1640 medium containing Glutamax-I, 10% heat inactivated fetal calf serum, 1% sodium pyruvate, 50 U/ml penicillin and streptomycin (all from Life Technologies, Paisley, United Kingdom), 50 ng/ml recombinant human GM-CSF, and 30 ng/ml recombinant human TNF-α (hereafter referred to as complete medium).

Flow Cytometry

Epidermal cells enriched in Fi LCs were washed once in RPMI 1640 supplemented with 10% fetal calf serum and resuspended in the same medium. The cells were incubated for 60 min at 37°C in the presence of either BFA (10 μg/ml), latrunculin A (12.5 μg/ml), cytochalasin D (10 μg/ml), or BFA and cytochalasin D (10 μg/ml each) and then cooled to 4°C. LCs were labeled by incubation with the anti-Langerin mAb DCGM4 (30 min at 4°C) and then, after two washes at 4°C, with the FITC-conjugated F(ab')$_2$ fraction of a sheep anti-mouse Ig antibody (30 min at 4°C). After washing, the cells were fixed and analyzed with a FACScan cytometer (BD Biosciences). IgG1 isotype controls were stained and examined simultaneously. The same procedure was used to analyze LCs cultured for 12, 24, or 48 h, in some experiments after pretreatment of the cells with either cytochalasin D (10 μg/ml), or BFA and cytochalasin D (10 μg/ml each).

Immunofluorescence Staining and Confocal Microscopy

Immunofluorescence microscopy of fixed permeabilized LCs was carried out as previously described (Saudrais *et al.*, 1998). Double staining with the anti-Langerin mAbs (DCGM4 or anti-lag) was performed as follows. After permeabilization with 0.05% saponin in phosphate-buffered saline containing 0.2% bovine serum albumin, the adherent cells were incubated with either DCGM4 or anti-lag

(1/1000 dilution), washed three times, and stained with Texas Red- or FITC-conjugated donkey anti-mouse IgG. The cells were washed again, fixed for 5 min in 3% paraformaldehyde, quenched for 10 min, and incubated with either FITC-conjugated anti-CD1a or CY3-anti-CD63 for 60 min, after which the coverslips were mounted in Mowiol. Double staining was also carried out using FITC-L243 (anti-HLA-DR$\alpha\beta$) or rabbit anti-EEA1 antiserum revealed with Texas Red-conjugated donkey anti-rabbit IgG F(ab')$_2$ fragments. In other experiments, the cells were pretreated with latrunculin A (12.5 μg/ml) or cytochalasin D (10 μg/ml), with or without BFA (10 μg/ml), for various times at 37°C before fixation, permeabilization, and double staining with 1) an anti-Langerin mAb revealed with Texas Red-conjugated donkey anti-mouse IgG and 2) either FITC-anti-CD1a or anti-Rab11. In control experiments, Fi LCs were incubated at 37°C for 1 h in the presence or absence of cytochalasin D (10 μg/ml), latrunculin A (12.5 μg/ml), or BFA (10 μg/ml). After fixation and permeabilization the cells were labeled simultaneously with an FITC-conjugated anti-CD1a mAb and phalloidine-TRITC, to study in LCs the effects of cytochalasin D and latrunculin A on the organization of actin filaments, or with CTR-433 followed by donkey anti-mouse TRITC and finally an FITC-conjugated anti-CD1a mAb to visualize in LCs the effects of BFA on Golgi distribution. Confocal laser scanning microscopy and immunofluorescence quantification were performed as previously described (Salamero et al., 1996) by using a Leica TCS4D confocal microscope (Leica Microsystems, Heidelberg, Germany).

Internalization of mAbs

Fi LCs or LCs cultured for 24, 48, or 72 h were allowed to adhere to glass coverslips precoated with poly-L-lysine. The cells were then incubated with the anti-Langerin mAb DCGM4 in RPMI 1640 (2 μg/ml) for 60 min at either 4°C or 19.5°C before fixation. Fi LCs were also incubated with DCGM4 in RPMI 1640 (2 μg/ml) for 30 min at 37°C, washed, and fixed either immediately or after incubation for 60 min at 37°C with cytochalasin D (10 μg/ml), or cytochalasin D and BFA (10 μg/ml each). In control experiments, Fi LCs were pretreated with cytochalasin D (10 μg/ml) or latrunculin A (12.5 μg/ml) for 60 min at 37°C before incubation, in the continuous presence of the drugs, for 30 min at 37°C with the anti-Langerin mAb and fixation. The fixed cells were permeabilized and double stained with FITC-anti-CD1a (5 μg/ml), anti-Rab11 (5 μg/ml), or rabbit anti-EEA1 antiserum (1/2000 dilution) revealed with Texas Red-conjugated donkey anti-rabbit IgG F(ab')$_2$ fragments.

Immunoelectron Microscopy

Fi epidermal cells were fixed in 1% paraformaldehyde and 0.1% glutaraldehyde in cacodylate buffer and processed for immunoelectron microscopy according to Mommaas et al. (1992). Ultrathin cryosections were successively incubated with an anti-Langerin mAb (1:300), rabbit anti-mouse IgG (1:200), and protein A-10-nm colloidal gold (1:400). The sections were then embedded in methylcellulose, stained with uranyl acetate, and examined under a Philips 410 electron microscope.

In other experiments, Fi epidermal cells were cooled to 19.5°C for 10 min, incubated for 60 min at the same temperature with 10-nm gold-labeled DCGM4 (final dilution 1:100), and either fixed immediately at 19.5°C or warmed to 37°C for 10, 20, or 30 min and then fixed at 37°C, before preparation of Epon sections. Fi epidermal cells and LCs cultured for 48 h were also incubated at 37°C for 45 min with cytochalasin D (10 μg/ml) or for 60 min with latrunculin A (12.5 μg/ml) and fixed at 37°C. In further experiments, the cells were preincubated for 30 min at 37°C with cytochalasin D (10 μg/ml), after which gold-labeled anti-CD1a or anti-Langerin was added for 15 or 30 min, still in the presence of cytochalasin D. Fi epidermal cells were also incubated with gold-labeled anti-Langerin for 35 min at 37°C, washed, and either fixed immediately or incubated for 45 min at 37°C with cytochalasin D (10 μg/ml), or cytochalasin D and BFA (10 μg/ml each), before fixation. Finally, Fi LCs were incubated with gold-labeled anti-CD1a for 35 min at 37°C and fixed for Epon sections.

Fixation was initiated by adding an equal volume of fixative solution, previously warmed to 19.5 or 37°C, to the cell suspension. The fixative solution contained 3% glutaraldehyde (Electron Microscopy Sciences, Euromedex, Strasbourg, France) and 2% sucrose in 0.1 M sodium cacodylate buffer (both Merck, Darmstadt, Germany) (305 mOsM, pH 7.3). After 5 min the mixture was centrifuged, the supernatant discarded, and the pellet resuspended and further fixed for 45 min at 19.5 or 37°C in the same fixative solution. The cells were then washed in 0.1 M sodium cacodylate buffer and postfixed for 1 h at 4°C with 1% osmium tetroxide (Merck) in the same buffer. After further washing in 0.1 M sodium cacodylate buffer, the cells were dehydrated in graded (50, 70, 80, 95, and 100%) ethanol solutions, incubated overnight in Epon (Electron Microscopy Sciences):absolute alcohol (1:1, vol/vol) and embedded in Epon. Ultrathin sections, stained with lead citrate (Leica, Bron, France) and uranyl acetate (Merck), were examined under a Philips CM 120 BioTwin electron microscope (120 kV).

In a final series of experiments, Fi epidermal cells and LCs cultured for 48 h were incubated at 37°C for 30 min with BFA (10 μg/ml) and then for 60 min in the presence of BFA (5 μg/ml) and HRP (10 mg/ml). The cells were subsequently processed according to Tooze and Hollinshead (1991) and Griffiths et al. (1989). After washing in phosphate-buffered saline and fixation with 0.5% glutaraldehyde in 0.1 M sodium cacodylate buffer pH 7.3 for 30 min at room temperature, the cells were washed in cacodylate buffer and incubated with DAB for 1 min. The HRP-DAB reaction was initiated by adding H$_2$O$_2$ to a final concentration of 0.01%. After 30 min in the dark, the reaction was terminated by washing several times in cacodylate buffer and the cells were postfixed in 1% osmium tetroxide, washed again in cacodylate buffer, and further processed as for conventional electron microscopy. Thick and ultrathin sections were examined under a Philips CM 120 BioTwin electron microscope (120 kV), in most cases without poststaining to allow better differentiation of the HRP-DAB reaction product.

RESULTS

Langerin Is Associated with Rab11$^+$/CD1a$^+$ Recycling Compartment

As an initial step, we characterized the distribution of Langerin in Fi LCs. Immunoelectron microscopy of ultrathin cryosections (Figure 1, A and B) revealed the presence of Langerin on the LC surface, in electron lucent compartments close to the cell surface suggestive of early endosomes, in BGs, and in other tubular and vesicular structures. Confocal microscopy (Figure 1, C–F) showed that internal Langerin molecules did not colocalize with the lysosomal markers Lamp-2 (Figure 1C) and Lamp-3/CD63 (our unpublished data) or with major histocompatibility complex class II molecules (our unpublished data). Rather, some colocalization between the internal pool of Langerin, as revealed by the anti-lag mAb, and the LC marker CD1a was evident in the pericentriolar area (Figure 1D). In another study carried out in the same cell type, we demonstrated that intracellular CD1a also colocalizes with Rab11 (Salamero et al., 2001), a small GTPase that specifically associates with the membrane of the endosomal recycling compartment (ERC) (Ullrich et al., 1996; Ren et al., 1998). Steady-state internal Langerin colocalized strongly with Rab11 in the ERC (Figure 1E) but poorly with EEA1, a marker of the early/sorting endosomes (Figure 1F) (Simonsen et al., 1998; Christoforidis et al., 1999; McBride et al., 1999). The steady-state localization of Lange-
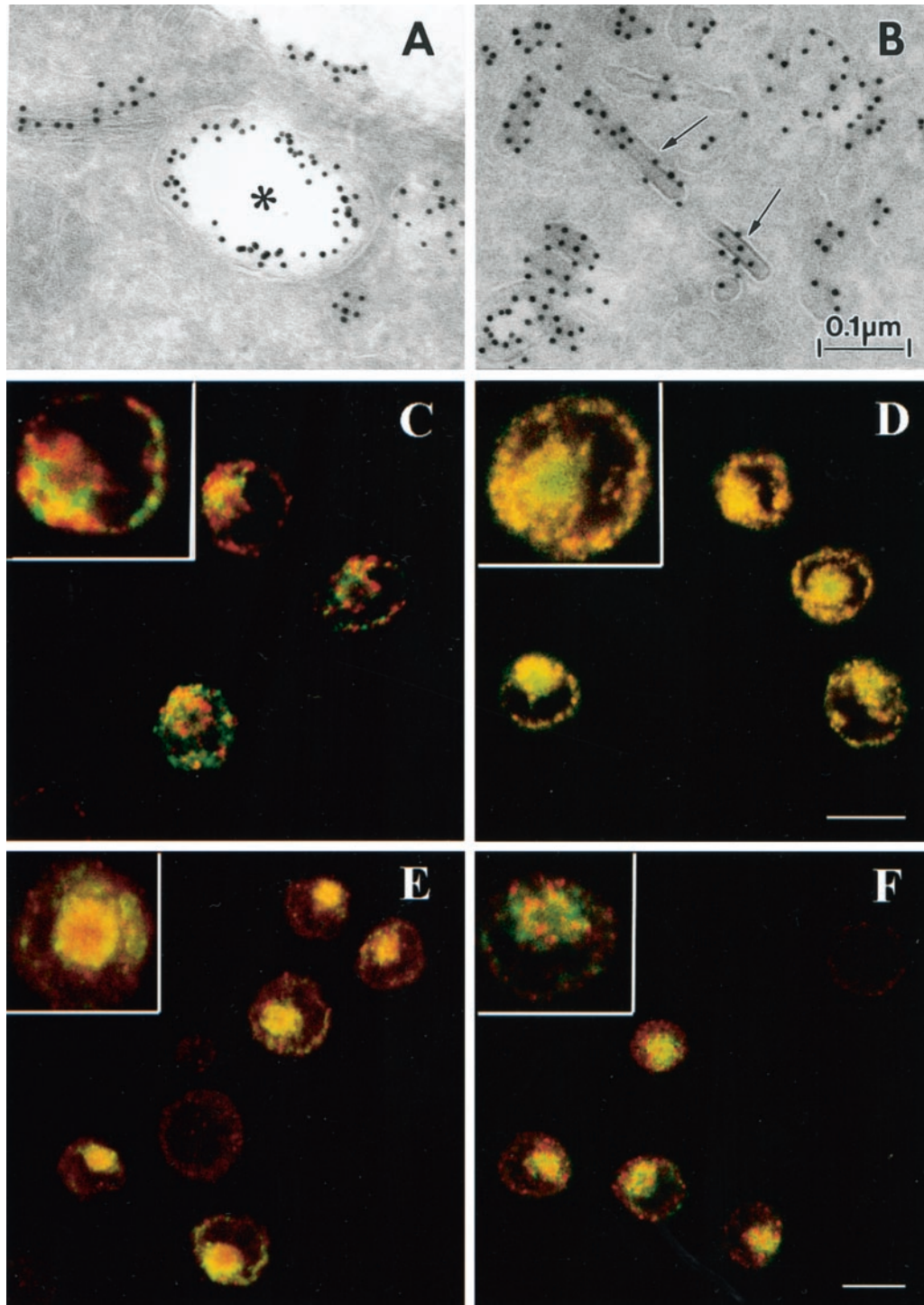
Figure 1. Steady-state distribution of Langerin molecules in Fi LCs. (A and B) Ultrathin cryosections of Fi LCs labeled for Langerin revealed the presence of this molecule at the LC surface (A), in an electron-lucent compartment close to the cell surface suggestive of an early endosome (star) (A), in BGs (arrows) (B), and in other tubular and vesicular structures (A and B). (C–F) Immunofluorescence staining was performed on cells fixed in paraformaldehyde and permeabilized with saponin as described in MATERIALS AND METHODS. In image (D), cells were incubated first with anti-lag antibody followed by Texas Red-conjugated donkey anti-mouse IgG and finally with FITC-conjugated anti-CD1a. In the remaining images, cells were simultaneously incubated with mouse-derived anti-lag and rabbit derived anti-Lamp (C), anti-Rab11 (E), and anti-EEA1 (F), before further incubation with donkey anti-mouse FITC and donkey anti-rabbit Texas Red. Higher magnification inserts are included to allow improved visualization of structural details. Bar, 10 μm.

rin was clearly different from that of CD1a, the latter being more equally distributed between the cell surface and internal membranes; however, this could be related to the dual role of the ERC as a sorting compartment for internalized proteins (Ghosh *et al.*, 1998; Mallet and Maxfield, 1999; Wilcke *et al.*, 2000) and as a storage reservoir for the regulated delivery of proteins to the plasma membrane (Johnson *et al.*, 2001). Hence, we next investigated whether Langerin, which is already known to endocytose in LCs (Valladeau *et al.*, 1999, 2000), cycles through the early endosomal pathway in a similar manner to CD1a molecules.

Cell Surface Langerin Internalizes through Classical Endocytic Structures before Reaching Birbeck Granules

To define the different endocytic structures through which cell surface Langerin traffics, cells were incubated in the presence of the anti-Langerin mAb DCGM4 over a range of temperatures. While at 4°C, DCGM4 labeled only the LC surface (Figure 2A), at 19.5°C it reached peripheral vesicular compartments distinct from the Rab11$^+$ (Figure 2B) and CD1a$^+$ (Figure 2C) ERC. The majority of these structures were identified as EEA1$^+$ early/sorting endosomes (Figure 2D). In contrast, incubation at 37°C allowed DCGM4 to reach the Rab11$^+$ (Figure 2F) and CD1a$^+$ (Figure 2E) ERC. No transport to late endosomal structures such as Lamp-2$^+$ or Lamp-3/CD63$^+$ compartments was detected at any time (our unpublished data). These results suggested that in Fi LCs, Langerin traffics between the plasma membrane, the early/sorting endosomes and the ERC, as might be expected for a recycling molecule. Using electron microscopy, we attempted to detail more precisely the organelles involved in this pathway and, in particular, the relationship between internalized Langerin and BGs. Fi LCs were incubated with DCGM4-Au for 60 min at 19.5°C and either immediately fixed at 19.5°C or warmed to 37°C for 10, 20, or 30 min before fixation. In LCs fixed at 19.5°C, temperature conditions known to inhibit cargo protein transfer from the early/sorting endosomes to the ERC (Ren *et al.*, 1998; Wilcke *et al.*, 2000), few gold particles were visible on the cell surface, most being concentrated in coated pits (Figure 3A). There was also labeling of coated vesicles (Figure 3A), tubular structures (Figure 3, A and B), and electron lucent compartments close to the cell surface, suggestive of early endosomes (Figure 3, C and D). As expected, progression of Langerin appeared to be blocked in these early endosomal-like structures, as illustrated by the accumulation of gold-labeled anti-Langerin mAb in these compartments (Figure 3D). Notably, no BGs were observed in continuity with the cell surface, nor was internalized DCGM4-Au detected in BGs (Figure 3D). In contrast, when LCs were further incubated at 37°C before fixation, gold labeling became apparent in the pericentriolar region, consistent with the results obtained by immunofluorescence. Although labeling persisted in vesicular and tubular structures (Figure 3H), the central linear striated density of pericentriolar BGs now contained gold particles (Figure 3, E–H). Interestingly, coated structures replete with DCGM4-Au were also present in the cell center (Figure 6G) and, in certain planes, appeared to be in continuity

with tubular structures (Figure 6G). Once again, no BGs were detected in continuity with the cell membrane. These observations illustrate that Langerin is internalized in Fi LCs by classical clathrin-coated receptor-mediated endocytosis. They also show that pericentriolar BGs and recycling compartments are accessible to anti-Langerin mAb, like anti-CD1a antibodies, in a temperature-dependent manner (Salamero *et al.*, 2001). Such findings indicate that Langerin behaves as a recycling molecule in Fi LCs and suggest that BGs could be part of or connected to the ERC.

Inhibition of Endocytosis Induces Redistribution of Intracellular Langerin and Appearance of "Birbeck Granule-like Structures" at Cell Surface

If Langerin undergoes a recycling process, inhibition of endocytosis under conditions where recycling to the plasma membrane is not affected should allow the internal pool to redistribute to the plasma membrane. Cytochalasin D and latrunculin A, known respectively to depolymerize and sequester F-actin filaments, have been shown to block the initial steps of endocytosis without affecting the recycling pathway in various cell types, including Fi LCs (Durrbach *et al.*, 1996; Lamaze *et al.*, 1997; Salamero *et al.*, 2001). Having confirmed by immunofluorescence their expected effects on filamentous actin in this cell type (our unpublished data), we found that latrunculin A (Figure 4B) and cytochalasin D (our unpublished data) were equally efficient in blocking the internalization of the mAb DCGM4 bound to Langerin at the surface of Fi LCs (compare Figure 4, B to A). Inhibition of endocytosis by either of these drugs resulted in approximately a 10-fold increase in cell surface Langerin expression, as measured by FACS analysis (Figure 4E). This was accompanied by a redistribution of the internal Langerin pool toward the cell surface, as seen on confocal microscopy images (compare Figure 4, C and D). Because this dramatic increase in cell surface expression could conceivably have been augmented by the export of newly synthesized Langerin molecules to the plasma membrane, we next examined the effect of BFA, a drug known to block the early biosynthetic/secretory pathway (Klausner *et al.*, 1992), on Langerin expression. We first confirmed the effect of BFA on the redistribution of the Golgi apparatus in LCs (our unpublished data). As expected, 1 h of treatment with BFA alone resulted in a diminution in cell surface Langerin expression (Figure 4E). This effect persisted when LCs were incubated with BFA in the presence of latrunculin A (our unpublished data) or cytochalasin D (Figure 4E), the previously described 10-fold increase in cell surface Langerin expression induced by these drugs being diminished by ~35%. It could be concluded from these results that part of the rise in cell surface Langerin expression induced by cytochalasin D or latrunculin A is due to a high level of synthesis of this molecule. Nevertheless, concomitant treatment with BFA still allowed a 6.5-fold increase in the cell surface expression of Langerin (Figure 4E). This "BFA-insensitive" increase most probably represents preexisting Langerin involved in a continuous endocytosis-recycling process.

Our next step was to examine the ultrastructural consequences of an inhibition of Langerin endocytosis on the distribution of BGs. Treatment with cytochalasin D or la-
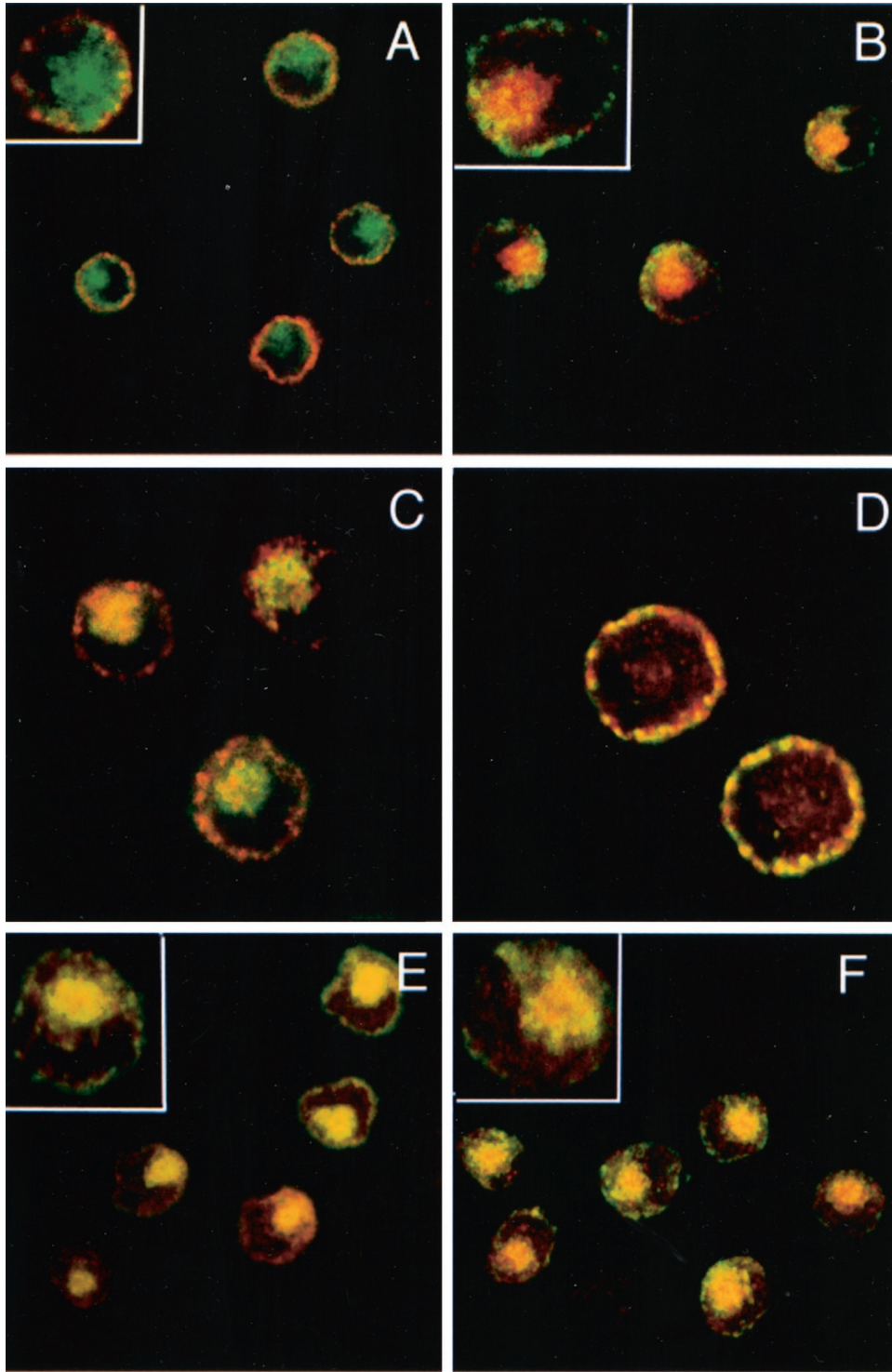
Figure 2. Internalization of the anti-Langerin mAb DCGM4. Fi LCs were incubated with the mouse anti-Langerin antibody DCGM4 for 1 h at either 4°C (A), 19.5°C (B–D), or 37°C (E and F). After rapid fixation in paraformaldehyde and permeabilization with saponin, the cells were incubated with donkey anti-mouse FITC IgG (B, D, and F) or donkey anti-mouse Texas Red IgG (A, C, and E), before counterstaining with FITC-conjugated anti-CD1a (A, C, and E) or either a rabbit anti-Rab11 (B and F) or anti-EEA1 (D) followed by donkey anti-rabbit Texas Red IgG. Bars, 10 μm.

trunculin A resulted in the appearance of abundant so-called "BG-like structures" appended to the cell membrane (Hanau *et al.*, 1988). Whereas in nontreated LCs, ~98% of BGs are not appended to the cell surface (Table 1), after 1 h of incubation with either drug, 58–59% of BGs become membrane appended. Addition of DCGM4-Au for the last 15 min of a 45-min treatment with cytochalasin D enabled us to identify the site of Langerin accumulation at the cell surface. The gold-labeled antibody was found in coated pits (Figure 5A) and BG-like structures (Figure 5, B–D). These latter were, for

the most part, enveloped in a coat, whether throughout their length or simply at their distal end, with gold particles along the length of the central linear striated density and/or in the coated distal end. A similar distribution was observed for CD1a, which, like Langerin, constitutively traffics through the early sorting/recycling endosomal pathway and accumulates at the LC surface, when endocytosis is blocked by cytochalasin D or latrunculin A (Figure 5, E–H) (Salamero et al., 2001). Thus, in the presence of cytochalasin D or latrunculin A, Langerin accumulates at the surface of LCs, where it is concentrated in coated BG-like structures and coated pits.

Internalized Langerin Recycles to Cell Surface

It is through studying the fate of internalized anti-Langerin antibody that we gained the best indication that this molecule is constantly recycling. Fi LCs incubated with the mAb DCGM4 for 30 min at 37°C and then chased in the absence of DCGM4 for up to 6 h demonstrated an accumulation of the antibody in the Rab11$^+$ recycling compartment (Figure 6A), without any significant loss of the fluorescent signal. However, treatment with cytochalasin D for 60 min at 37°C resulted in a relocalization of preinternalized DCGM4 from this compartment to the cell surface (Figure 6B). On the basis of these results, we next incubated Fi LCs with DCGM4-Au for 35 min at 37°C, washed the cells, and either fixed them immediately or further incubated them for 45 min at 37°C in the presence of cytochalasin D before fixation. In cells fixed immediately, the cell surface was weakly labeled, with most gold particles concentrated in coated pits (Figure 6D). Labeling accumulated in the pericentriolar area (Figure 6G) where it was found in vesicular and tubular structures, in the central linear striated density of BGs, and in coated organelles that were sometimes in continuity with tubular structures (Figure 6G). Chase in the presence of cytochalasin D resulted in a relocalization of this labeling to the cell surface (Figure 6E), with almost none remaining in the pericentriolar area (Figure 6H). Although pericentriolar BGs remained, none contained gold particles. In contrast, many of the numerous BG-like structures and coated pits visible at the cell surface were labeled (Figure 6E). These structures were frequently coated, whether along all their length or simply at their distal end, the gold particles lying along the central linear striated density and/or in the coated distal end. These findings show that anti-Langerin mAbs travel from the periphery of the cell to the pericentriolar area, where they label Rab11$^+$ compartments and BGs, before subsequently returning to the cell surface. This not only confirms the recycling of Langerin at the ultrastructural level but also demonstrates that the pericentriolar BGs belong to this pathway.

Brefeldin A Partially Inhibits Recycling of Internalized Langerin

Ultrastructural studies of the internalization of the anti-Langerin mAb DCGM4 revealed (Figure 6G) the existence of numerous coated structures filled with gold particles in the pericentriolar area. In addition, confocal microscopy studies showed that internalized DCGM4 accumulated in the Rab11$^+$ ERC (Figure 2, E and F). These two findings suggested that the coated structures might represent transport intermediates involved in Langerin recycling. Small G proteins of the ADP-ribosylation factor (Arf) family recruit and assemble protein complexes, leading to the formation of cellular coats. This requires their interaction with Arf exchange factors that catalyze the exchange of GDP for GTP, a process that can be inhibited by BFA (Donaldson et al., 1992a,b). The resultant inhibition of coat formation interrupts the membrane traffic regulatory functions they normally carry out (Lippincott-Schwartz et al., 1991; Klausner et al., 1992). In view of the known inhibitory effect of BFA on coat formation and the predominance of coated structures in the pericentriolar area, we reexamined the influence of BFA on Langerin recycling. LCs were first charged with DCGM4 for 30 min at 37°C (Figure 6A) and then chased for 60 min at 37°C in the presence of cytochalasin D alone or cytochalasin D and BFA. Addition of BFA led to the retention of at least part of the internalized Langerin in the recycling compartment (compare Figure 6, C and B). At the ultrastructural level LCs took on an intermediate appearance. At the cell surface, a picture was obtained similar to that described after a chase in the presence of cytochalasin D alone, namely, labeling of BG-like structures and coated structures (Figure 6F). In contrast, the pericentriolar labeling, involving vesicular and tubular structures and the central linear striated density of BGs, was not unlike that seen after internalization of gold-labeled DCGM4 in untreated cells (compare Figure 6, I and G), except that there was no evidence of coating of these structures.

Brefeldin A Induces Fusion of Birbeck Granules with Other Components of Endocytic Pathway

Through its effect on coat formation, BFA has also been shown to induce fusion and redistribution of the membranes of the early endocytic pathway and the trans-Golgi network (TGN), resulting in a continuous tubular network (Lippincott-Schwartz et al., 1991; Wood et al., 1991). Thus, we next examined the effect of BFA on the relationship between BGs and the endosomal system. Epidermal cells were incubated at 37°C for 30 min with BFA (5 μg/ml) and then for 60 min in the presence of both BFA and HRP (10 mg/ml). Control cells were incubated for 60 min with HRP alone, a period sufficiently long to saturate the tubular endosomes and BGs with HRP (our unpublished data). The presence of BFA led to the appearance of elongated HRP-positive BGs, which were frequently connected with tubular and vesicular structures. Whereas in some places the labeled BGs seemed to lie at the extremities of the tubular structures (Figure 7, A and A'), in other areas they clearly constituted an integral part of a tubular network (Figure 7, C–E).

Thus, it would appear that BFA on the one hand reduces the recycling of internalized Langerin and, on the other, promotes interconnections between BGs and components of the endosomal system. In fact, such tubular networks were also occasionally observed in untreated cells (Figure 8A). The internalization of a gold-labeled anti-CD1a mAb to these network structures indicates that they correspond to the recycling compartment. Interestingly, some of the CD1a-positive tubular networks and neighboring BGs were coated (Figure 8, B–E). These results suggest that intracellular BGs form an integral part of the recycling pathway in Fi LCs.
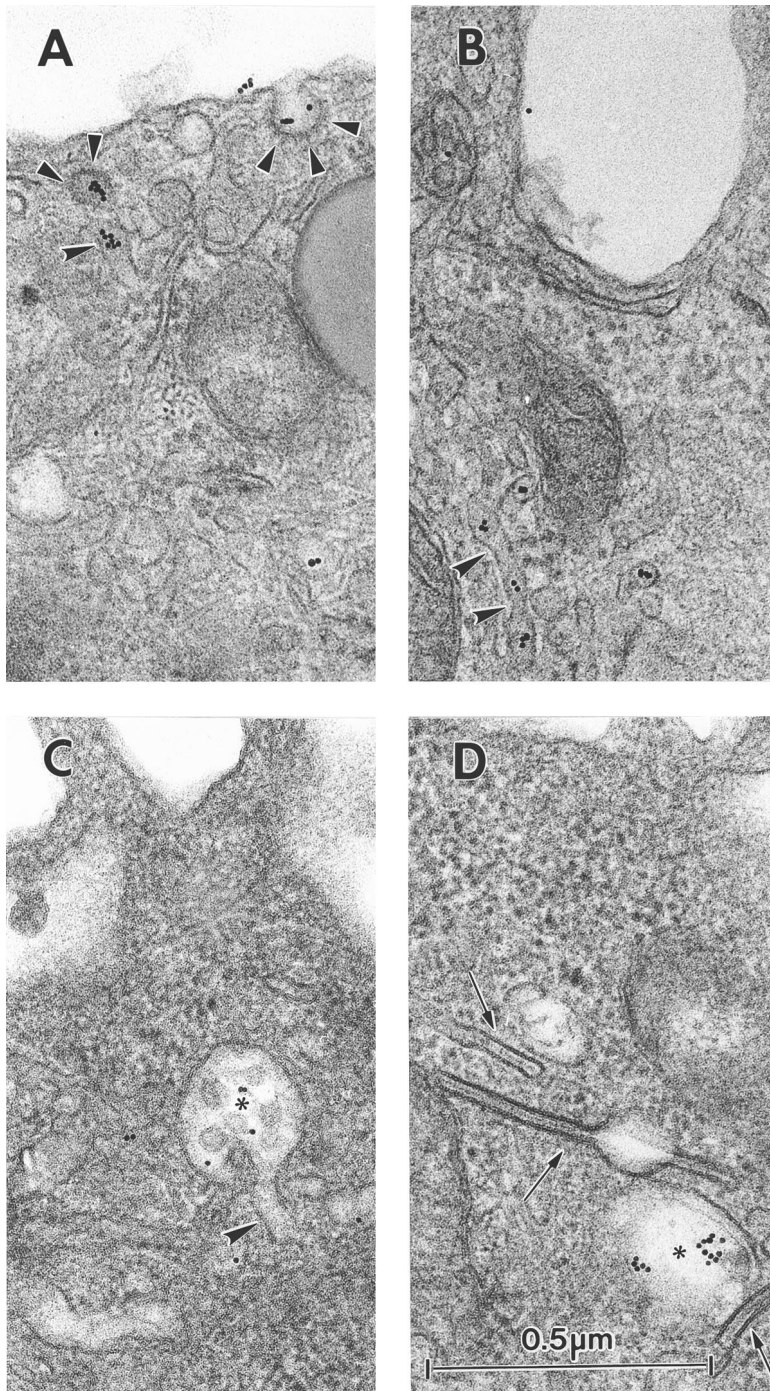
Figure 3. Internalization of the gold-labeled anti-Langerin mAb DCGM4. Fi LCs were incubated with DCGM4-Au for 1 h at 19.5°C and either immediately fixed at 19.5°C (A–D) or warmed to 37°C for 30 min before fixation (E–H). LCs incubated for 1 h at 19.5°C had few gold particles visible on the cell surface, most being concentrated in coated pits (arrowheads) (A). Labeling was also present in coated vesicles (arrowheads) (A), tubular structures (curved arrowheads) (A and B), and electron lucent compartments close to the cell surface suggestive of early endosomes (star) (C and D). Progression of Langerin appeared to be blocked in the early endosomal-like structures, as illustrated in D. Note the absence of labeling in the three intracytoplasmic BGs (arrows) visible in D. (A–D are at the same magnification.) When LCs were further incubated at 37°C before fixation, gold labeling became apparent in the central linear striated density of some of the pericentriolar (E and F) and perinuclear (G and H) BGs (arrows). (H) Gold-labeling was still present in electron lucent compartments (star), now located in the perinuclear region, and in tubular structures (curved arrowheads). (E–H are at the same magnification.) C, centriole; Nu, nucleus.

Langerhans Cell Maturation Abolishes Langerin Cycling and Results in Depletion of Internal Langerin and Birbeck Granules

Because many of the properties of LCs depend on their state of maturation, we examined the influence of the maturation of LCs on their ability to internalize Langerin. Although flow cytometry (Figure 9G) indicated that maturation had little overall effect on the cell surface expression of Langerin,

confocal microscopy revealed a change in its distribution (compare Figure 9, B and C, with A). After 48 h of maturation, the internal Langerin pool was markedly reduced or absent. At this time point, confocal images taken with fixed acquisition parameters (Salamero *et al.*, 1996) showed a significant decrease in the intensity of total cell anti-Langerin fluorescence (Figure 9H). Moreover, the anti-Langerin mAb rapidly lost its ability to spontaneously internalize in LCs
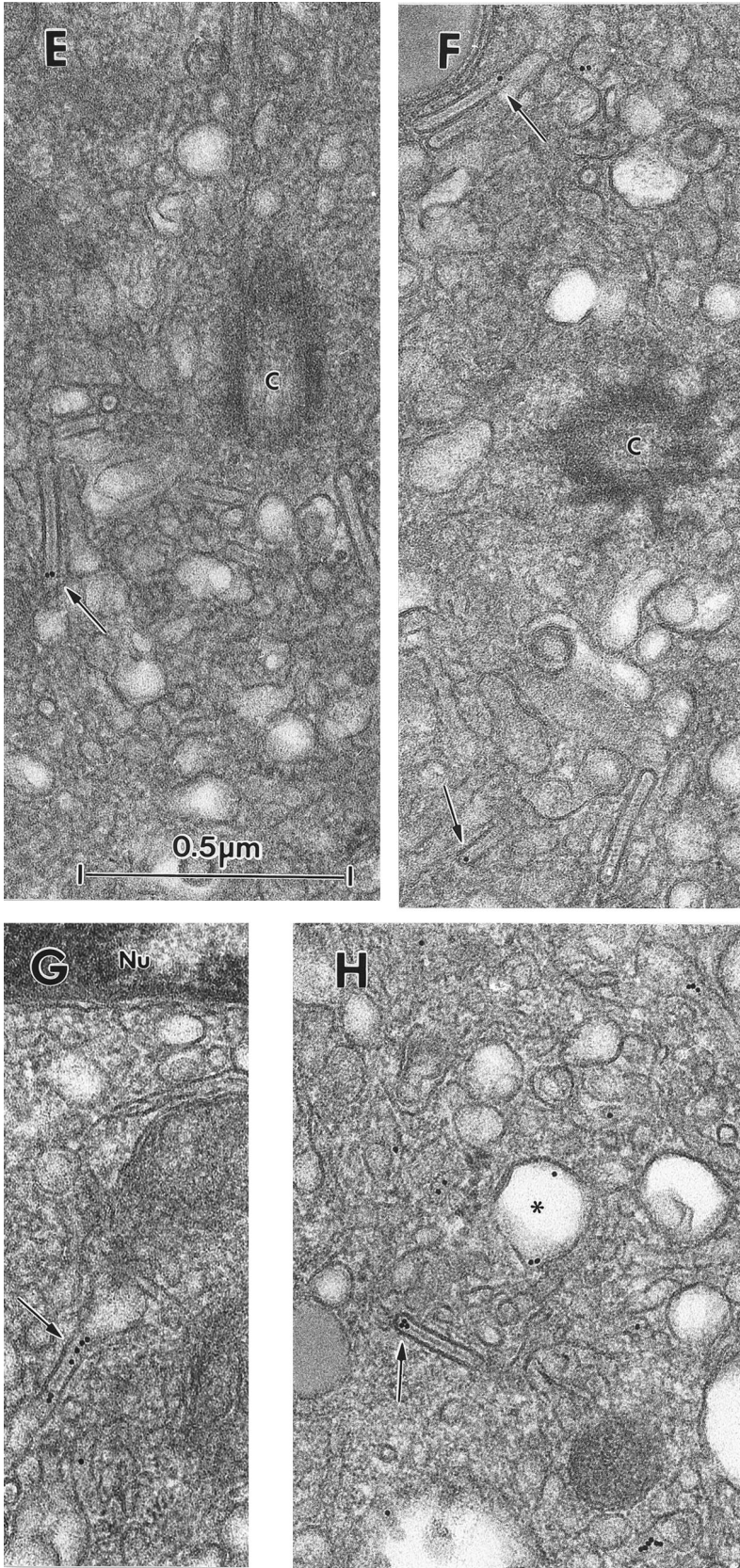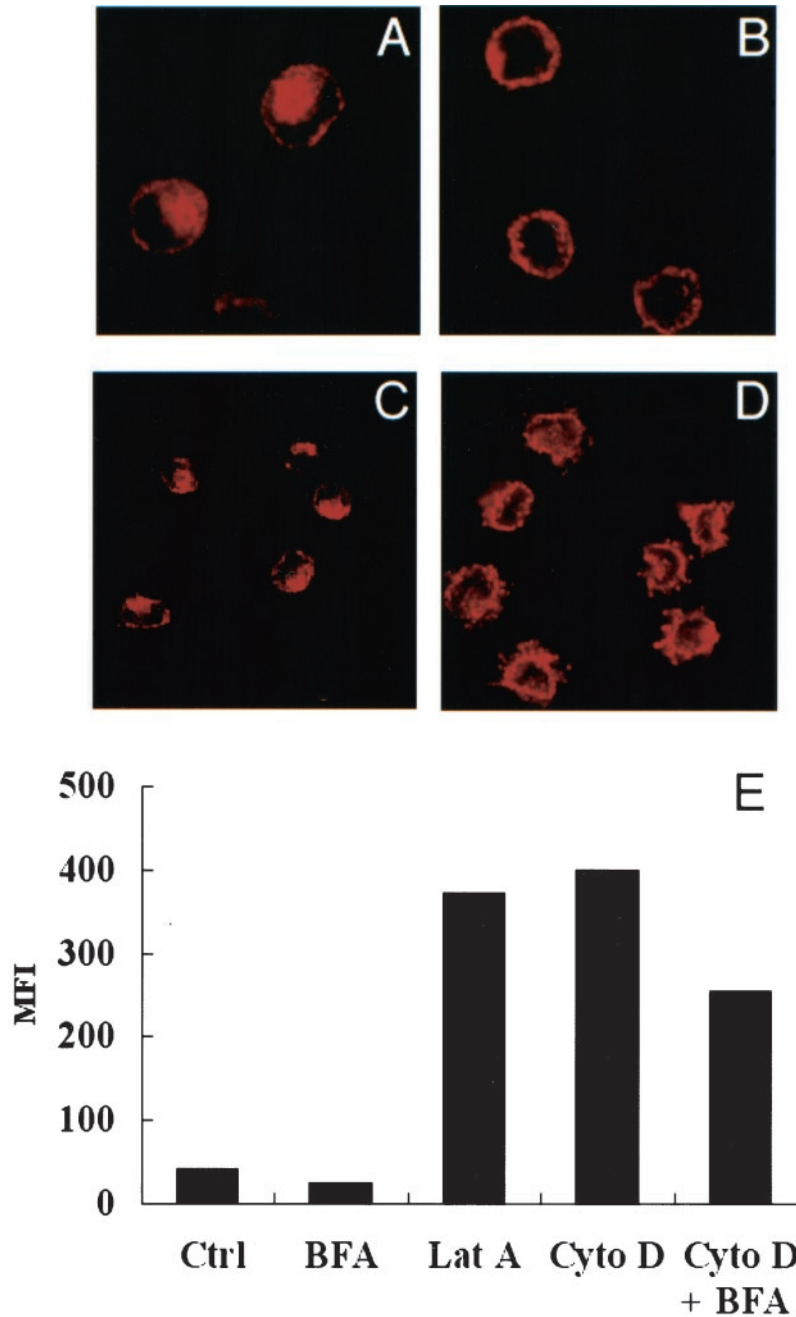
Figure 3 (cont).

Figure 4. Inhibition of endocytosis induces the redistribution of Langerin at the plasma membrane. (A) Fi LCs were incubated with the anti-Langerin antibody DCGM4 for 1 h at 37°C. (B) Cells were pretreated with cytochalasin D (10 μg/ml) for 30 min at 37°C, before incubation for 1 h with DCGM4 at 37°C in the continuous presence of the drug. After fixation and permeabilization, the cells were incubated with donkey anti-mouse Texas Red IgG and analyzed by confocal microscopy. Fi LCs were incubated at 37°C for 1 h without drug treatment (C) or in the presence of cytochalasin D before permeabilization and labeling for Langerin (D). (E) Fi LCs were incubated with cytochalasin D (10 μg/ml), latrunculin A (12.5 μg/ml), BFA (10 μg/ml) or a combination of these drugs for 1 h at 37°C and Langerin surface expression measured by FACS scan. Results shown are the mean of data from five different LC donors. MFI, mean fluorescence intensity.

undergoing maturation (compare Figure 9, E and F, to D). Because Langerin continuously recycles in LCs, this loss of the capacity to internalize could explain the depletion of the internal Langerin pool in mature LCs. In mature cells, inhibition of endocytosis with cytochalasin D/latrunculin A no longer resulted in an accumulation of Langerin at the cell surface, nor did BFA partly block recycling of Langerin to the cell surface (Figure 9G). At the ultrastructural level, cytochalasin D or latrunculin A, both of which induced a 60% increase in the number of BG-like structures in Fi LCs, no longer triggered the appearance of BG-like structures appended to the cell membrane, nor did BFA induce the forma-

tion of continuous endosomal networks (our unpublished data). Compared with their immature counterparts, mature LCs were characterized by a smaller number of short rod like BGs (our unpublished data), dispersed among autophagolysosomes in the pericentriolar area, as previously described (Stössel *et al.*, 1990).

DISCUSSION

Although their presence in LCs was first described 40 yr ago, the origin and function of BGs has remained elusive. Two

Table 1. Effect of the inhibition of endocytosis on BG distribution To analyse the localization of BGs, cells were first incubated for 1 h at 37° in the chosen conditions then prepared for immunoelectron microscopy as described in MATERIALS AND METHODS. Counts represent summation of serial median profiles (cytochalasin D, 15; latrunculin A, 11).

	No. (%) of BGs in indicated location		
	Intracytoplasmic	Appended to cell surface	Total
Control	222 (98)	5 (2)	227 (100)
Cytochalasin D	96 (41)	133 (59)	226 (100)
Control	110 (99)	1 (1)	111 (100)
Latrunculin A	40 (42)	54 (58)	94 (100)

opposing theories have been proposed as to their function. The first suggests that BGs could function as alternative endocytotic structures, specific to LCs (Tarnowski and Hashimoto, 1967; Hashimoto, 1971; Ishii *et al.*, 1984; Takahashi and Hashimoto, 1985; Takigawa *et al.*, 1985; Bartosik, 1992). However, in our hands and under physiological conditions, BGs appended to the cell surface were an exceptional finding, as previously reported by Wolff (1972) and Stössel *et al.* (1990). Moreover, we found no evidence that BGs participate in the internalization of Langerin, suggested to be one of their essential constituents. Unlike in the physiological state, "open ended" (Elema and Atmosoerodjo-Briggs, 1984) BG-like structures appended to the cell membrane were rapidly induced by treating Fi LCs with cytochalasin D or latrunculin A, irrespective of the presence of an anti-Langerin mAb. One possible explanation for these results would be that BGs represent a transient endocytic intermediate that can no longer be pinched off the cell membrane in the presence of these drugs. However, not only BG-like structures were seen under these conditions but also
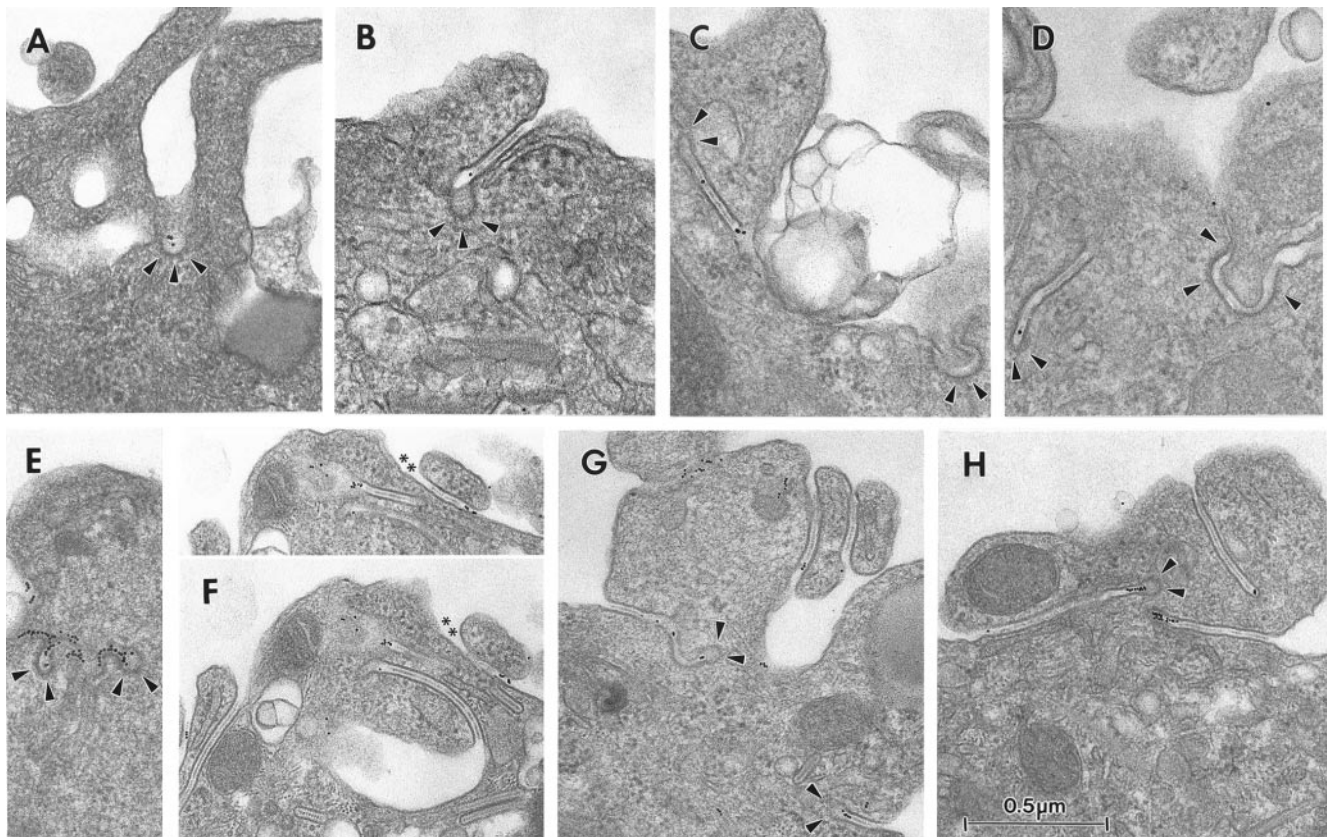

Figure 5. Inhibition of endocytosis induces the appearance of "BG-like structures" and clathrin-coated structures labeled with anti-Langerin mAb. Fi LCs were incubated for 30 min at 37°C in the presence of cytochalasin D (10 μg/ml), before addition of DCGM4-Au (A–D) or anti-CD1a-Au (E–H) for a further 15 min. Gold particles accumulated in coated pits (arrowheads) (A) and in BG-like structures (B–D). These latter had coated pits (arrowheads) at their cytoplasmic terminal end (B) or were enveloped in a coat at their distal end (arrowheads) (C and D). Gold particles were present along the central linear striated density of the BG-like structures (B and C) or at their coated distal end (D). Note the presence of a coat (arrowheads) along the BG-like structure in the right hand part of B and D. There are more CD1a gold particles in the coated pits (arrowheads) (E) and BG-like structures (F and G) than in the equivalent labeling for Langerin, as predicted by the differences in surface expression of the two molecules. CD1a-Au also concentrated in the coated distal end (arrowheads) of BG-like structures (G and H). Note the numerous BG-like structures apparent in F, G, and H. The superior aspect of the LC in F contains two regions labeled with gold particles (∗∗) whose "BG-like" nature was demonstrated by tilting (+25°) (F, top).
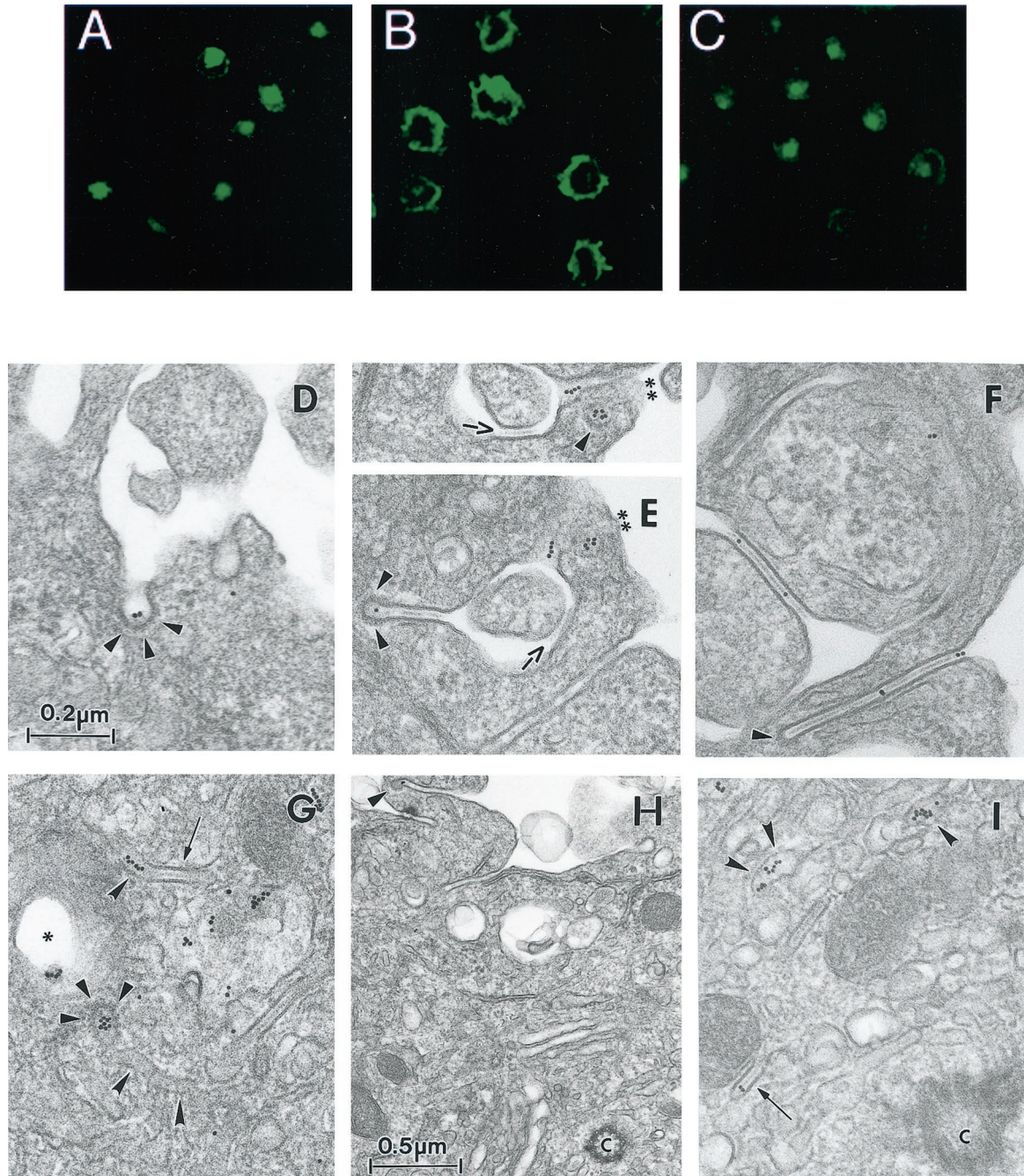
Figure 6. Brefeldin A partially inhibits the effect of cytochalasin D. Fi LCs were incubated with DCGM4 for 30 min at 37°C, the cells were washed and further incubated for 1 h without drug treatment (A), in the presence of cytochalasin D (B), or in the presence of both cytochalasin D and BFA (C). Cells were then fixed and permeabilized and staining revealed with donkey anti-mouse FITC IgG. In a similar manner, Fi LCs were incubated with DCGM4-Au for 35 min at 37°C, washed, and either fixed immediately (D and G) or further incubated for 45 min at 37°C in the presence of cytochalasin D alone (E and H) or both cytochalasin D and BFA (F and I) before fixation. (D and G) Immediate fixation revealed DCGM4-Au–labeled coated structures (arrowheads) at the LC surface (D). Labeling also accumulated in the cell center (G), with gold particles visible in a tubular structure (curved arrowheads) continuous with a BG (arrows) and in a coated structure (arrowheads) in continuity with a tubular structure (curved arrowheads). Cytochalasin D treatment resulted in a relocalization of the intracellular labeling to the cell surface. Many of the numerous BG-like structures are labeled with DCGM4-Au and are coated at their distal end (arrowheads). The region labeled with gold particles in E (∗∗) was revealed by tilting (+23°) to be a coated pit (arrowheads) (E, top). This also reveals that the arrowed region in E is in fact a BG-like structure. The low-magnification image (H) demonstrates the reduced intracellular labeling in these conditions. After addition of BFA, many gold-labeled BG-like structures coated at their distal end (arrowheads) are visible at the LC surface (F). Note the retention of internalized DCGM4-Au in the pericentriolar area (I), particularly in BGs (arrow) and tubular structures (curved arrowheads) (C, centriole). D–F and G and I are at the same magnification.
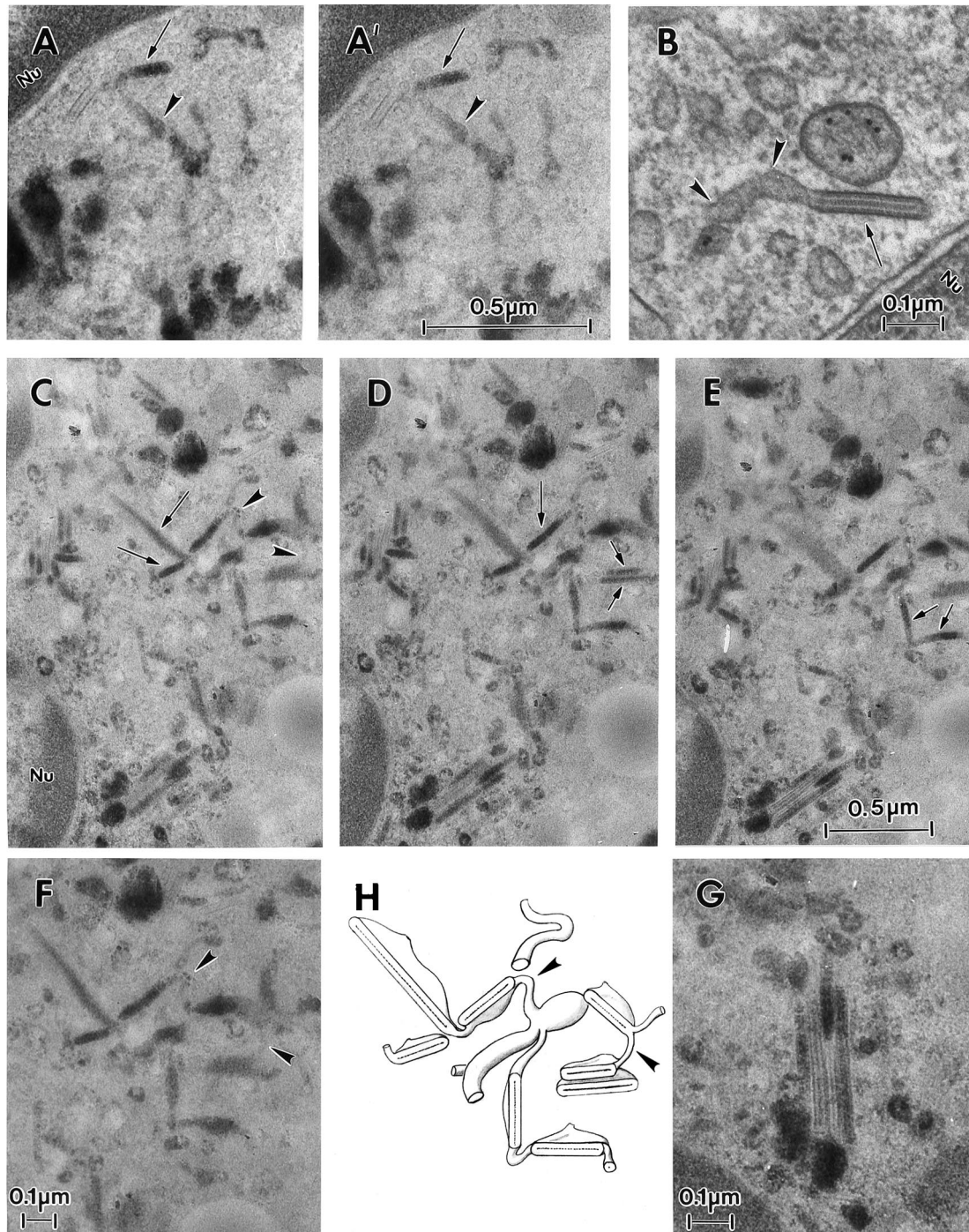
Figure 7. BFA induces fusion of BGs with tubular endosomes. A thin section of an Fi LC incubated at 37°C for 35 min in the presence of the gold-conjugated anti-CD1a mAb (B) demonstrates continuity between a medium-sized tubule (curved arrowheads) and a BG (arrow). Thick sections of Fi LCs incubated at 37°C for 30 min with 5 μg/ml BFA and then for 60 min in the presence of both BFA and 10 mg/ml HRP are visible on A, A', C–F, and G. A and A' display the same perinuclear (Nu) region seen at different angles (A, tilt −25°; A', tilt −35°). Note the continuity between an HRP-positive BG (arrows) and an element of the tubular endosome (curved arrowheads) and the presence of an unlabeled BG. In images C–E a single region is viewed from different angles (C, tilt +25°; D, tilt +10°; E, tilt −10°). Note the presence of many HRP-labeled BGs (arrows) and of interconnecting tubular structures (closed arrowheads with a white border). F is a higher magnification of C to illustrate interconnections (curved arrowheads) between BGs. G is a higher magnification of the lower left region of E, showing four heterogenously labeled BGs adopting a "pancake" arrangement. Note the effect of the angle of tilt on the appearance of the HRP labeling and the features of the BGs. H is a schematic representation of the complex tubular network seen in C–E. C–E are at the same magnification.
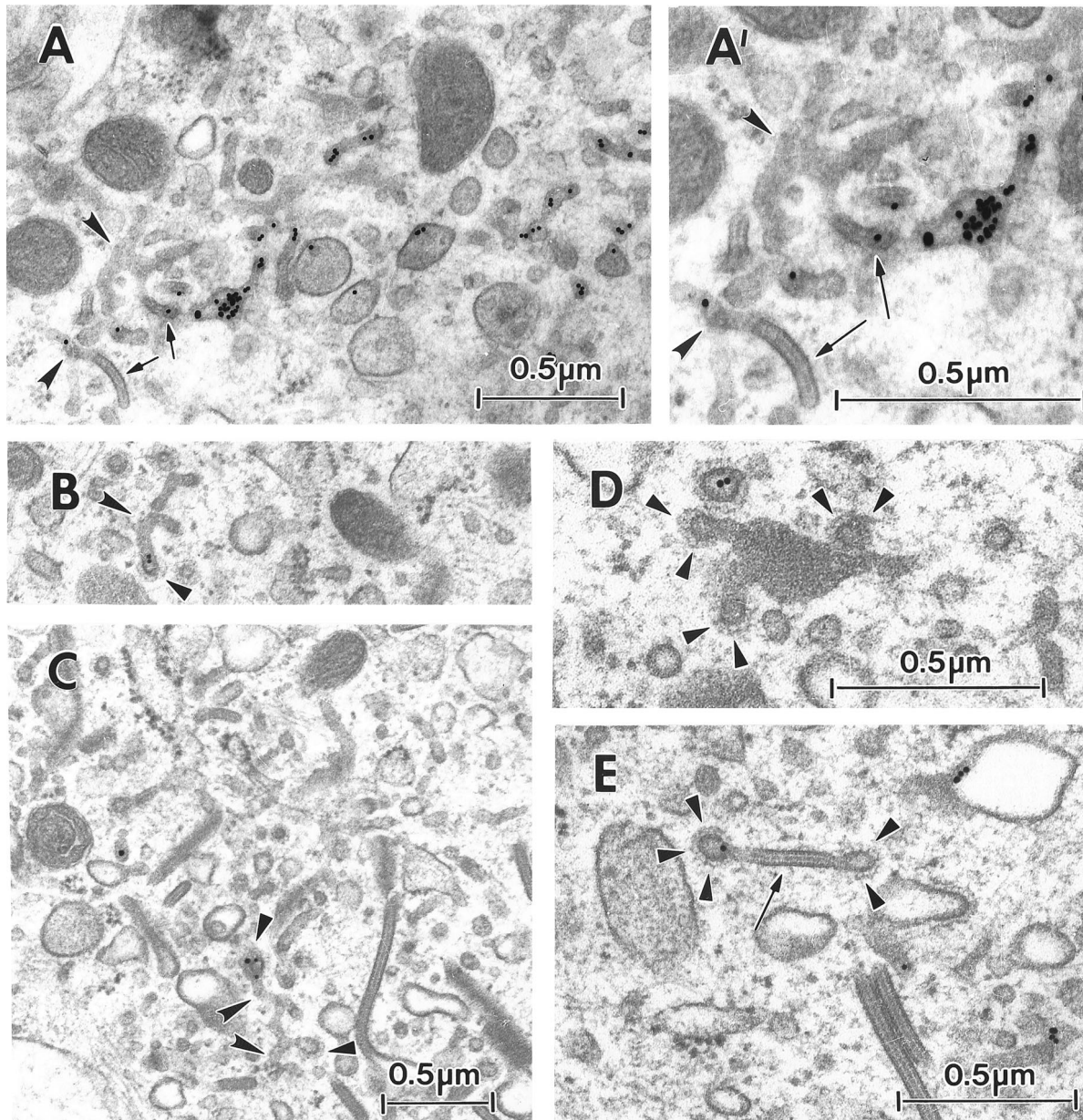
Figure 8. Ultrastructural particularities of the early endodomal network. Fi LCs were incubated at 37°C, for 35 min, in the presence of anti-CD1a-Au. (A and A′) The branched tubules (curved arrowheads) visible in A, and at a higher magnification in A′, appear to be gold-labeled and in continuity with BGs (arrows). In B and C, the bulbous ends of gold-labeled branches of the tubular networks (curved arrowheads) appear to be coated (arrowheads). D shows the characteristic square lattice aspect of a BG connected to three coated structures (arrowheads). Finally, in E, a BG cut perpendicular to the BG plane is connected to two coated structures, one of which is gold-labeled (arrowheads).

a large number of coated pits, which were labeled by gold-conjugated anti-Langerin mAb, consistent with the recognized effect of these drugs on classical receptor-mediated endocytosis (Durrbach *et al.*, 1996; Lamaze *et al.*, 1997; Salamero *et al.*, 2001). In addition, many of the BG-like structures were clathrin coated, or had labeled coated pits at their cytoplasmic terminal end. These findings indicate first that Langerin endocytosis is mediated by a classical clathrin-coated pathway, regardless of whether the plasma membrane is linear or folded, as in the characteristic zipped formation of BG-like structures and, second, that BGs are not endocytotic structures.

The second proposed theory regarding BG function is that they could represent secretory structures formed in the Golgi area and involved in transport of cargo molecules to the cell membrane. The disappearance of BGs from the
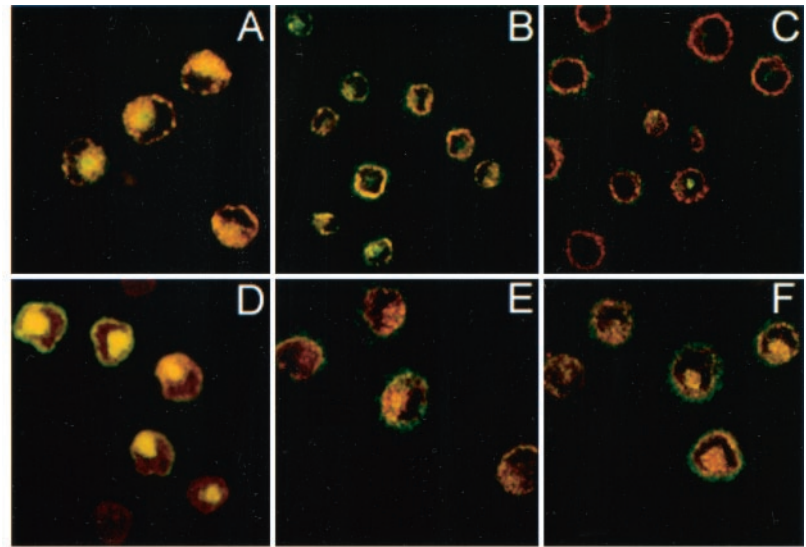
Figure 9. Langerin recycling is altered in mature Fi LCs. Permeabilized Fi LCs were double immunolabeled for Langerin (red staining) and CD1a (green staining) either at T0 (A) or after 24 h (B) or 48 h (C) of culture with GM-CSF and TNF-α. Fi LCs were incubated with the anti-Langerin antibody DCGM4 for 1 h at 37°C at T0 (D) or after 24 h (E) or 48 h (F) of culture with GM-CSF and TNF-α. Langerin staining was revealed with donkey anti-mouse Texas Red IgG before counterstaining performed with FITC-conjugated anti-CD1a mAb. (G) Confocal series (8 consecutive sections, each separated by 0.5 μm) of at least 50 different cells at each time point were taken using fixed acquisition parameters. The total anti-Langerin fluorescence intensity of reconstituted stacks of these series was then quantified by image analysis. This analysis was performed at each time point both at the steady state (diagonal lines) and after internalization of DCGM4 antibody (black shading). (H) Cell surface Langerin expression was measured by FACS scan at T0, T24, and T48 in Fi LCs incubated for 1 h at 37°C without drugs (gray shading), with cytochalain D at 10 μg/ml (white shading), or with a combination of cytochalasin D and BFA both at 10 μg/ml (black shading). MFI, mean fluorescence intensity.
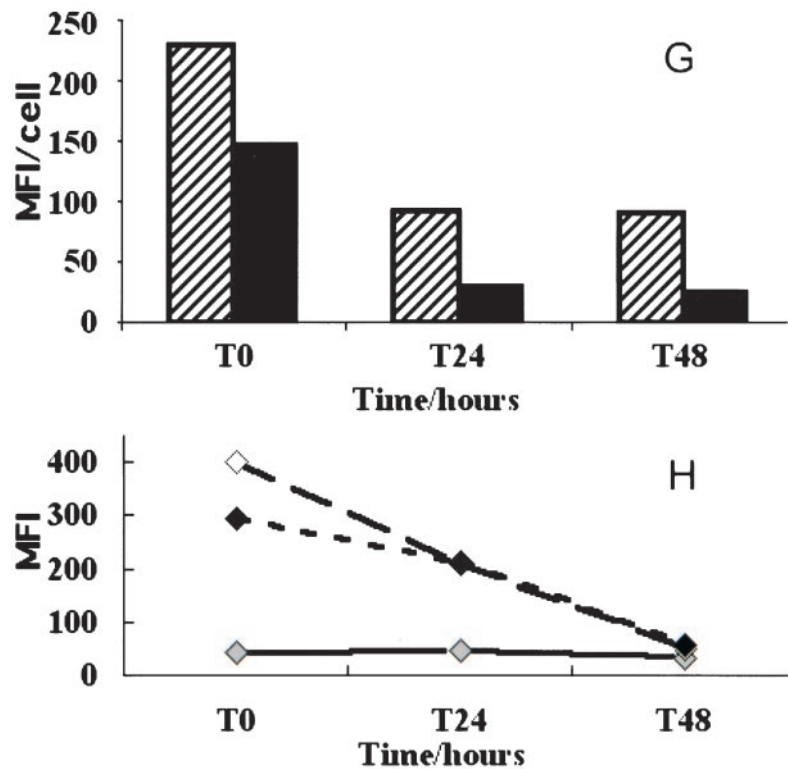
pericentriolar area and concomitant appearance of BG-like structures at the cell membrane after cytochalasin D or latrunculin A treatment could signify that BGs act as transport intermediates "driving" Langerin, and perhaps other molecules, from internal membranes to the cell surface. On arrival at the cell surface such BGs would fuse with the plasma membrane, in a similar manner to synaptic vesicles originating from the early endosomal pathway (Desnos *et al.*, 1995). Unzipping would follow, allowing delivery of their molecular content to the cell surface.

However, immunoelectron microscopy revealed BGs in continuity with tubular structures and also occasionally as part of early endosomal tubular networks in the pericentriolar area, networks which became manifest after treatment with BFA. In addition, after internalization at 19.5°C and temperature shift to 37°C, Langerin was found both in the recycling compartments and in pericentriolar BGs. Thus it is apparent that BGs may simply represent membrane domains of tubular recycling endosomes, the morphology of which has been modified by the formation of molecular

bridges. In this context, the elongated tubular configuration of the recycling compartment (Hopkins *et al.*, 1994) could enable two membrane leaflets to come into close apposition, facilitating the generation of BGs. In contrast, such membrane interaction might not occur in early sorting endosomes because of their vesicular shape.

The predominance of BGs in the ERC could also be explained if the molecules responsible for their formation transiently accumulate in this compartment during their traffic. We have demonstrated this to be the case for Langerin both in the steady state and after internalization of anti-Langerin antibody. Moreover, when Langerin was redistributed and concentrated at the plasma membrane, by inhibition of endocytosis, numerous BG-like structures appended to the cell surface became apparent and, in mature LCs, when the internal pool of Langerin is depleted, there is a concomitant reduction in the number of BGs. Given its exclusive expression in LCs and the primacy of this relationship, it appears likely that BGs arise through the interaction of Langerin molecules with one another and/or other ligands. We propose the hypothesis that when a "minimal zipping concentration" of these molecules is reached in the ERC, close membrane apposition is induced and BGs arise in preexisting tubular structures. Similarly, BG-like structures form in membrane folds when Langerin is redistributed and concentrated at the plasma membrane.

Indeed, evidence exists to support this interpretation. First, BGs can form within ER membranes in murine fibroblasts transfected with human Langerin cDNA (Valladeau *et al.*, 2000). In this nonphysiological situation, the endoplasmic reticulum membranes are likely to contain high levels of newly synthesized Langerin even in the steady state. Second, in CD34$^+$-derived LCs, which are characteristically clumped, we were able to generate BG-like structures between the plasma membranes of neighboring cells by treatment with cytochalasin D (our unpublished data). Finally, unzipping of BGs by EDTA induces the appearance of vesiculo-tubular structures (Andersson *et al.*, 1988), suggesting that divalent cations are important in the bridging of BG membranes, which is significant as Langerin is a transmembrane type II Ca^{2+}-dependent lectin (Valladeau *et al.*, 2000). These findings substantiate our belief that BGs represent morphological modifications of preexisting membranes, rather than specific transport intermediates.

Nonetheless, other endosomal membrane proteins could also be implicated in the genesis of BGs. Hanau *et al.* (1991), for example, were able to induce the formation of such structures from the dilated elements of the surface-connected canalicular system of EDTA-treated human platelets. These morphological changes were dependent on the appearance of integrin α_{IIb} homopolymers, acting as bridges between adjacent membranes of the surface-connected canalicular system and leading to their "zipping" (Gachet *et al.*, 1993).

The results of BFA treatment provide further insight into this unusual membrane-trafficking process. BFA partially inhibited the effects of cytochalasin D treatment, namely, the redistribution of Langerin from intracellular pools, recycling of internalized anti-Langerin antibodies from the ERC and disappearance of gold-labeled anti-Langerin mAbs from the pericentriolar membrane structures, including BGs. This effect would appear to be mediated through inhibition of Arf-dependent coat formation, a recognized consequence of BFA treatment (Chardin and McCormick, 1999). Thus, although coated structures labeled with internalized anti-Langerin or anti-CD1a mAbs were seen in the pericentriolar area in the absence of drug treatment, after addition of BFA the labeled, fused tubular endosomes and pericentriolar BGs were no longer coated. In contrast, the BG-like structures appended to the cell surface generated by cytochalasin D or latrunculin A treatment remained coated with clathrin even in the presence of BFA. Hence, these latter coats must differ in composition from those of the pericentriolar BGs and tubular recycling endosomes. It is most probable that they represent AP-2 clathrin coats, because AP-2 recruitment is Arf1 independent (D'Souza-Schorey *et al.*, 1995) and therefore unaffected by BFA (Robinson and Kreis, 1992). This difference in coat composition provides persuasive evidence that the composition of BG-like structures differs from that of the pericentriolar BGs.

Although the presence of clathrin coats on endosomes and their ability to segregate proteins have been previously described (Louvard *et al.*, 1983; Le Borgne *et al.*, 1996; Stoorvogel *et al.*, 1996; Mallard *et al.*, 1998), the transport pathways in which they are involved remain obscure. Clathrin coats have been implicated in the transport of cargo proteins from early endosomes to an unknown destination, perhaps the plasma membrane (Stoorvogel *et al.*, 1996) and by a retrograde pathway from early endosomes to the TGN (Mallard *et al.*, 1998), the route taken being dependent upon the nature of the adaptor protein complexes. On reaching the TGN, these cargo proteins may either pursue a retrograde pathway to the endoplasmic reticulum (Johannes *et al.*, 1997) or resume the secretory route to the cell surface. Thus, TGN46 and furin, for example, recycle continuously between the plasma membrane, sorting endosomes, the ERC, and the TGN. The kinetics of their traffic is nonetheless such that in the steady state these proteins are highly concentrated in the TGN (Ghosh *et al.*, 1998; Mallet and Maxfield, 1999). Likewise, there exist cycling proteins that are dynamically retained within organelles related to the early endosomal compartments (Johnson *et al.*, 1993; Marsh *et al.*, 1995; Johnson *et al.*, 1998; Mayor *et al.*, 1998), such as GPI-linked proteins and the transmembrane insulin-regulated aminopeptidase, which are concentrated in the ERC of fibroblasts (Mayor *et al.*, 1998; Johnson *et al.*, 2001).

Therefore, the steady-state concentration of a protein within a compartment can result from a "dynamic" retention, achieved by slow recycling from the compartment to the cell surface coupled with rapid retrieval back to that compartment. Whether the steady-state localization of Langerin in the ERC of LCs is due to a slow kinetic of recycling from subdomains of the ERC to the LC surface remains to be established. The transient accumulation of Langerin in these subdomains would generate the "minimal zipping concentration" required for BG formation, hence, BGs could serve as a regulated Langerin reservoir within the ERC. Studies are currently underway to identify the adaptor proteins present in the BFA-sensitive coated structures that appear in continuity with internal BGs and tubular recycling endosomes. This should provide further insight into the nature of BGs.

Although Langerin seems to be involved in the biogenesis of BGs, its functional role in LCs remains obscure. Interest-

ingly, Langerin possesses a single carbohydrate recognition domain with a glutamate-proline-asparagine motif predicting mannose type specificity (Valladeau *et al.*, 2000), a potentially important property because LCs lack classical mannose receptors (Mommaas *et al.*, 1999). Ligands of Langerin have yet to be described, however, it could serve as a receptor for the capture of specific microbial antigens by this unique population of antigen-presenting cells. One can only speculate as to which antigen-presenting molecules Langerin might deliver bound antigen; however, on the basis of our results, CD1a is a potential target-presenting molecule. We have demonstrated that endocytosed Langerin and CD1a molecules share a common intracellular fate in LCs, traveling through identical intracellular compartments, including pericentriolar BGs. Moreover, endocytosis and recycling of both molecules is arrested by LC maturation (Salamero *et al.*, 2001). Because BGs form where Langerin accumulates in the ERC and are depleted when LCs are activated, they could in this context, serve as a loading compartment and/or a membrane reservoir for antigens before LC maturation.

ACKNOWLEDGMENTS

REFERENCES

Andersson, L., Bartosik, J., Bendsoe, N., Malmström, A., Mikulowska, A., Warfvinge, K., Andersson, A., and Falck, B. (1988). Formation and unzipping of Birbeck granules in vitro. In: The Langerhans Cell (ed. J. Thivolet and D. Schmitt), Paris: Les Editions INSERM/John Libbey Eurotext Ltd, 185–191.

Bartosik, J. (1992). Cytomembrane-derived Birbeck granules transport horseradish peroxidase to the endosomal compartment in the human Langerhans cells. J. Invest. Dermatol. *99*, 53–58.

Birbeck, M.S., Breathnach, A.S., and Everall, J.D. (1961). An electron microscope study of basal melanocytes and high-level clear cells (Langerhans cells) in vitiligo. J. Invest. Dermatol. *37*, 51–63.

Chardin, P., and McCormick, F. (1999). Brefeldin A: the advantage of being uncompetitive. Cell *97*, 153–155.

Christoforidis, S., McBride, H.M., Burgoyne, R.D., and Zerial, M. (1999). The Rab5 effector EEA1 is a core component of endosome docking. Nature *397*, 621–625.

Desnos, C., Clift-O'Grady, L., and Kelly, R.B. (1995). Biogenesis of synaptic vesicles in vitro. J. Cell Biol. *130*, 1041–1049.

Donaldson, J.G., Cassel, D., Kahn, R.A., and Klausner, R.D. (1992a). ADP-ribosylation factor, a small GTP-binding protein, is required for binding of the coatomer protein beta-COP to Golgi membranes. Proc. Natl. Acad. Sci. USA *89*, 6408–6412.

Donaldson, J.G., Finazzi, D., and Klausner, R.D. (1992b). Brefeldin A inhibits Golgi membrane-catalyzed exchange of guanine nucleotide onto ARF protein. Nature *360*, 350–352.

D'Souza-Schorey, C., Li, G., Colombo, M.I., and Stahl, P.D. (1995). A regulatory role for ARF6 in receptor-mediated endocytosis. Science *267*, 1175–1178.

Durrbach, A., Louvard, D., and Coudrier, E. (1996). Actin filaments facilitate two steps of endocytosis. J. Cell Sci. *109*, 457–465.

Elema, J.D., and Atmosoerodjo-Briggs, J.E. (1984). Langerhans cells and macrophages in eosinophilic granuloma. An enzyme-histochemical, enzyme-cytochemical, and ultrastructural study. Cancer *54*, 2174–2181.

Fithian, E., Kung, G., Goldstein, G., Rubenfeld, M., Fenoglio, C., and Edelson, R.L. (1981). Reactivity of Langerhans cells with hybridoma antibody. Proc. Natl. Acad. Sci. USA *78*, 2541–2544.

Gachet, C., Hanau, D., Spehner, D., Brisson, C., Garaud, J.-C., Schmitt, D.A., Ohlmann, P., and Cazenave, J.-P. (1993). $\alpha IIb\beta 3$ integrin dissociation induced by EDTA results in morphological changes of the platelet surface-connected canalicular system with differential location of the two separate subunits. J. Cell Biol. *120*, 1021–1030.

Ghosh, R.N., Mallet, W.G., Soe, T.T., McGraw, T.E., and Maxfield, F.R. (1998). An endocytosed TGN38 chimeric protein is delivered to the TGN after trafficking through the endocytic recycling compartment in CHO cells. J. Cell Biol. *142*, 923–936.

Griffiths, G., Back, R., and Marsh, M. (1989). Quantitative analysis of the endocytic pathway in baby hamster kidney cells. J. Cell Biol. *109*, 2703–2720.

Hanau, D., Fabre, M., Schmitt, D.A., Garaud, J.-C., Pauly, G., and Cazenave, J.-P. (1988). Appearance of Birbeck granule-like structures in anti-T6 antibody-treated human epidermal Langerhans cells. J. Invest. Dermatol. *90*, 298–304.

Hanau, D., Fabre, M., Schmitt, D.A., Lepoittevin, J.-P., Stampf, J.-L., Grosshans, E., Benezra, C., and Cazenave, J.-P. (1989). ATPase and morphological changes in Langerhans cells induced by epicutaneous application of a sensitizing dose of DNFB. J. Invest. Dermatol. *92*, 689–694.

Hanau, D., Fabre, M., Schmitt, D.A., Stampf, J.-L., Garaud, J.-C., Bieber, T., Grosshans, E., Benezra, C., and Cazenave, J.-P. (1987). Human epidermal Langerhans cells internalize by receptor-mediated endocytosis T6 (CD1 "NA1/34) surface antigen: Birbeck granules are involved in the intracellular traffic of the T6 antigen. J. Invest. Dermatol. *89*, 172–177.

Hanau, D., Gachet, C., Ohlmann, P., Brisson, C., Fabre, M., and Cazenave, J.-P. (1991). Ultrastructural similarities between epidermal Langerhans cell Birbeck granules and the surface-connected canalicular system of EDTA-treated human blood platelets. J. Invest. Dermatol. *97*, 756–762.

Hashimoto, K. (1971). Langerhans cell granule. An endocytotic organelle. Arch. Dermatol. *104*, 148–160.

Hopkins, C.R., Gibson, A., Shipman, M., Strickland, D.K., and Trowbridge, I.S. (1994). In migrating fibroblasts, recycling receptors are concentrated in narrow tubules in the pericentriolar area, and then routed to the plasma membrane of the leading lamella. J. Cell Biol. *125*, 1265–1274.

Ishii, M., Terao, Y., Kitajima, J.-I., and Hamada, T. (1984). Sequential production of Birbeck granules through adsorptive pinocytosis. J. Invest. Dermatol. *82*, 28–29.

Jasmin, B.J., Cartaud, J., Bornens, M., and Changeux, J.P. (1989). Golgi apparatus in chick skeletal muscle: changes in its distribution during end plate development and after denervation. Proc. Natl. Acad. Sci. USA *86*, 7218–7222.

Johannes, L., Tenza, D., Antony, C., and Goud, B. (1997). Retrograde transport of KDEL-bearing B-fragment of Shiga toxin. J. Biol. Chem. *272*, 19554–19561.

Johnson, L.S., Dunn, K.W., Pytowski, B., and McGraw, T.E. (1993). Endosome acidification and receptor trafficking: bafilomycin A1 slows receptor externalization by a mechanism involving the receptor's internalization motif. Mol. Biol. Cell *4*, 1251–1266.

Johnson, A.O., Lampson, M.A., and McGraw, T.E. (2001). A dileucine sequence and a cluster of acidic amino acids are required for dynamic retention in the endosomal recycling compartment of fibroblasts. Mol. Biol. Cell *12*, 367–381.

Johnson, A.O., Subtil, A., Petrush, R., Kobylarz, K., Keller, S.R., and McGraw, T.E. (1998). Identification of an insulin-responsive, slow endocytic recycling mechanism in Chinese hamster ovary cells. J. Biol. Chem. *273*, 17968–17977.

Kashihara, M., Ueda, M., Horiguchi, Y., Furukawa, F., Hanaoka, M., and Imamura, S. (1986). A monoclonal antibody specifically reactive to human Langerhans cells. J. Invest. Dermatol. *87*, 602–607.

Klareskog, L., Malmnas-Tjezrnlund, U., and Peterson, P.A. (1977). Epidermal Langerhans cells express Ia antigens. Nature *268*, 248–250.

Klausner, R.D., Donaldson, J.G., and Lippincott-Schwartz, J. (1992). Brefeldin A: insights into the control of membrane traffic and organelle structure. J. Cell Biol. *116*, 1071–1080.

Kripke, M.L., Munn, C.G., Jeevan, A., Tang, J.M., and Bucana, C. (1990). Evidence that cutaneous antigen presenting cells migrate to regional lymph nodes during contact sensitization. J. Immunol. *145*, 2833–2838.

Lamaze, C., Fujimoto, L.M., Yin, H.L., and Schmid, S.L. (1997). The actin cytoskeleton is required for receptor-mediated endocytosis in mammalian cells. J. Biol. Chem. *272*, 20332–20335.

Le Borgne, R., Griffiths, G., and Hoflack, B. (1996). Mannose 6-phosphate receptors and ADP-ribosylation factors cooperate for high affinity interaction of the AP-1 Golgi assembly proteins with membranes. J. Biol. Chem. *271*, 2162–2170.

Lippincott-Schwartz, J., Yuan, L., Tipper, C., Amherdt, M., Orci, L., and Klausner, R.D. (1991). Brefeldin A's effects on endosomes, lysosomes, and the TGN suggest a general mechanism for regulating organelle structure and membrane traffic. Cell *67*, 601–616.

Louvard, D., Morris, C., Warren, G., Stanley, K., Winkler., F., and Reggio, H. (1983). A monoclonal antibody to the heavy chain of clathrin. EMBO J. *2*, 1655–1664.

Mallard, F., Antony, C., Tenza, D., Salamero, J., Goud, B., and Johannes, L. (1998). Direct pathway from early/recycling endosomes to the Golgi apparatus revealed through the study of shiga toxin B-fragment transport. J. Cell Biol. *143*, 973–990.

Mallet, W.G., and Maxfield, F.R. (1999). Chimeric forms of furin and TGN38 are transported with the plasma membrane in the trans-Golgi network via distinct endosomal pathways. J. Cell Biol. *146*, 345–359.

Marsh, E.W., Leopold, P.L., Jones, N.L., and Maxfield, F.R. (1995). Oligomerized transferrin receptors are selectively retained by a lumenal sorting signal in a long-lived endocytic recycling compartment. J. Cell Biol. *129*, 1509–1522.

Martinez, O., Schmidt, A., Salamero, J., Hoflack, B., Roa, M., and Goud, B. (1994). The small GTP-binding protein rab6 functions in intra-Golgi transport. J. Cell Biol. *127*, 1575–1588.

Mayor, S., Sabharanjak, S., and Maxfield, F.R. (1998). Cholesterol-dependent retention of GPI-anchored proteins in endosomes. EMBO J. *17*, 4626–4638.

McBride, H.M., Rybin, V., Murphy, C., Giner, A., Teasdale, R., and Zerial, M. (1999). Oligomeric complexes link Rab5 effectors with NSF and drive membrane fusion via interactions between EEA1 and syntaxin 13. Cell *98*, 377–386.

Mommaas, A.M., Mulder, A.A., Jordens, R., Out, C., Tan, M.C., Cresswell, P., Kluin, P.M., and Koning, F. (1999). Human epidermal Langerhans cells lack functional mannose receptors and a fully developed endosomal/lysosomal compartment for loading of HLA class II molecules. Eur. J. Immunol. *29*, 571–580.

Mommaas, A.M., Wijsman, M.C., Mulder, A.A., van Praag, M.C.G., Vermeer, B.J., and Koning, F. (1992). HLA class II expression on human epidermal Langerhans cells in situ: up-regulation during the elicitation of allergic contact dermatitis. Hum. Immunol. *34*, 99–106.

Moll, H., Fuchs, H., Blank, C., and Röllinghoff, M. (1993). Langerhans cells transport *Leishmania major* from the infected skin to the draining lymph node for presentation to antigen-specific T cells. Eur. J. Immunol. *23*, 1595–1601.

Ren, M., Xu, G., Zeng, J., De Lemos-Chiarandini, C., Adesnic, M., and Sabatini, D. (1998). Hydrolysis of GTP on rab11 is required for the direct delivery of transferrin from the pericentriolar recycling compartment to the cell surface but not from sorting endosomes. Proc. Natl. Acad. Sci. USA *95*, 6187–6192.

Robinson, M.S., and Kreis, T.E. (1992). Recruitment of coat proteins onto Golgi membranes in intact and permeabilized cells: effects of brefeldin A and G protein activators. Cell *69*, 129–138.

Rowden, G., Lewis, M.G., and Sullivan, A.K. (1977). Ia antigen expression on human epidermal Langerhans cells. Nature *268*, 247–248.

Salamero, J., Bausinger, H., Mommaas, A.M., Lipsker, D., Proamer, F., Cazenave, J.-P., Goud, B., de la Salle, H., and Hanau, D. (2001). CD1a molecules traffic through the early recycling endosomal pathway in human Langerhans cells. J. Invest. Dermatol. *116*, 401–408.

Salamero, J., Le Borgne, R., Saudrais, C., Goud, B., and Hoflack, B. (1996). Expression of major histocompatibility complex class II molecules in HeLa cells promotes the recruitment of AP-1 Golgi-specific assembly proteins on Golgi membranes. J. Biol. Chem. *271*, 30318–30321.

Saudrais, C., Spehner, D., de la Salle, H., Bohbot, A., Cazenave, J.-P., Goud, B., Hanau, D., and Salamero, J. (1998). Intracellular pathway for the generation of functional MHC class II peptide complexes in immature human dendritic cells. J. Immunol. *160*, 2597–2607.

Schuler, G., Romani, N., Stössel, H., and Wolff, K. (1991). Structural organization and biological properties of Langerhans cells. In: Epidermal Langerhans Cells (ed. G. Schuler), Boca Raton, FL: CRC Press, Inc., 87–137.

Simonsen, A., Lippe, R., Christoforidis, S., Gaullier, J.M., Brech, A., Callaghan, J., Toh, B.H., Murphy, C., Zerial, M., and Stenmark, H. (1998). EEA1 links PI(3)K function to Rab5 regulation of endosome fusion. Nature *394*, 494–498.

Stoorvogel, W., Oorschot, V., and Geuze, H.J. (1996). A novel class of clathrin-coated vesicles budding from endosomes. J. Cell Biol. *132*, 21–33.

Stössel, H., Koch, F., Kämpgen, E., Stöger, P., Lenz, A., Heufler, C., Romani, N., and Schuler, G. (1990). Disappearance of certain acidic organelles (endosomes and Langerhans cell granules) accompanies loss of antigen processing capacity upon culture of epidermal Langerhans cells. J. Exp. Med. *172*, 1471–1482.

Takahashi, S., and Hashimoto, K. (1985). Derivation of Langerhans cell granules from cytomembrane. J. Invest. Dermatol. *84*, 469–471.

Takigawa, M., Iwatsuki, K., Yamada, M., Okamoto, H., and Imamura, S. (1985). The Langerhans cell granule is an adsorptive endocytic organelle. J. Invest. Dermatol. *85*, 12–15.

Tarnowski, W.T., and Hashimoto, K. (1967). Langerhans'cell granules in histiocytosis X. The epidermal Langerhans'cell as a macrophage. J. Invest. Dermatol. *96*, 298–304.

Tooze, J., and Hollinshead, M. (1991). Tubular early endosomal networks in AtT20 and other cells. J. Cell Biol. *115*, 635–653.

Ullrich, O., Reinsch, S., Urbé, S., Zerial, M., and Parton, R. (1996). Rab11 regulates recycling through the pericentriolar recycling endosome. J. Cell Biol. *135*, 913–924.

Valladeau, J., *et al*. (1999). The monoclonal antibody DCGM4 recognizes Langerin, a protein specific of Langerhans cells, and is rapidly internalized from the cell surface. Eur. J. Immunol. *29*, 2695–2704.

Valladeau, J., *et al*. (2000). Langerin, a novel C-type lectin specific to Langerhans cells, is an endocytic receptor that induces the formation of Birbeck granules. Immunity *12*, 71–81.

Wilcke, M., Johannes, L., Galli, T., Mayau, V., Goud, B., and Salamero, J. (2000). Rab11 regulates the compartmentalization of early endosomes required for efficient transport from early endosomes to the trans-Golgi-network. J. Cell Biol. *151*, 1207–1220.

Wolff, K. (1967). The fine structure of the Langerhans cell granule. J. Cell Biol. *35*, 468–477.

Wolff, K. (1972). The Langerhans cells. In: Current Problems in Dermatology, vol. 4, (ed. J.W.H. Mali), Basel: Karger, 100–103.

Wood, S.A., Park, J.E., and Brown, W.J. (1991). Brefeldin A causes a microtubule-mediated fusion of the trans-Golgi network and early endosomes. Cell *67*, 591–600.

Zelickson, A.S. (1966). Granule formation in the Langerhans cell. J. Invest. Dermatol. *47*, 498–502.